Appraising Multinuclear Cu²⁺ Structure Formation in Cu-CHA SCR Catalysts via Low-T Dry CO Oxidation with Modulated NH₃ Solvation

Umberto Iacobone,[a] Isabella Nova,[a] Enrico Tronconi,*[a] Roberta Villamaina,[b] Maria Pia Ruggeri,[b] Jillian Collier,[b] and David Thompsett[b]

Cu^{2+} ions ($ZCu^{2+}(OH)^-$, Z_2Cu^{2+}) are regarded as the NH₃-SCR (SCR = selective catalytic reduction) active site precursors of Cu-exchanged chabazite (CHA) which is among the best available catalysts for the abatement of NO_x from Diesel engines. During SCR operation, copper sites undergo reduction (Reduction half-cycle, RHC: $Cu^{2+} \rightarrow Cu^+$) and oxidation (Oxidaton half-cycle, OHC: $Cu^+ \rightarrow Cu^{2+}$) semi cycles, whose associated mechanisms are still debated. We recently proposed CO oxidation to CO_2 as an effective method to probe the formation of multinuclear Cu^{2+} species as the initial low-T RHC step. NH₃ pre-adsorption determined a net positive effect on the CO_2 production: by solvating $ZCu^{2+}(OH)^-$ ions, ammonia enhances their mobility, favoring their coupling to form binuclear complexes which can catalyze the reaction. In this work, dry CO oxidation experiments, preceded by modulated NH₃ feed phases, clearly showed that CO_2 production enhancements are correlated with the extent of Cu^{2+} ion solvation by NH₃. Analogies with the SCR-RHC phase are evidenced: the NH_3-Cu^{2+} presence ensures the characteristic dynamics associated with a second order kinetic dependence on the oxidized Cu^{2+} fraction. These findings provide novel information on the NH₃ role in the low-T SCR redox mechanism and on the nature of the related active catalyst sites.

Introduction

Air pollution is a growing worldwide concern, and abatement technologies are required to cope with increasingly stringent emission regulations. Nitrogen oxides (NO_x) are a family of gaseous polluting compounds originating from combustion processes, and the NH₃/urea selective catalytic reduction (SCR) is the leading, state-of-the-art technology for their control from vehicular lean Diesel engines.[1,2] Cu^{2+} ions are considered the deNOx active site precursors in Cu-exchanged chabazite-type zeolites (Cu-CHA), currently among the best performing catalysts for this application due to their superior hydrothermal stability, resistance to hydrocarbon poisoning and an effective SCR activity in a wide temperature range.[3–5] In the last decade, several studies have been conducted to disclose the fundamental and mechanistic features of the SCR chemistry. However,

many open issues still remain, in particular related to the nature of the Cu intermediates.[6–8] Several works converged to highlight the SCR process redox nature, which relies on two half cycles concurrently proceeding during common working conditions: a reduction and an oxidation half cycle (RHC and OHC), where the ions are reduced to Cu^+ and re-oxidized back to Cu^{2+}, respectively.[6,9–12] The existence of two kinds of isolated Cu^{2+} ions located in different zeolite structure positions has been probed by a combination of transient methods, spectroscopic techniques and molecular dynamics,[2,8,13] namely $ZCu^{2+}(OH)^-$, located in the eight-membered ring of the CHA cage, where the two positive charges of copper are balanced by one coordination with the local framework-Al (Z) and by a hydroxyl group $(OH)^-$; and conversely, Z_2Cu^{2+}, which is bonded twice to the zeolite in the six-membered ring. Furthermore, the relative populations of these two species are affected by several factors, such as hydrothermal aging as well as the SiO_2/Al_2O_3 and the Cu/Al ratio of Cu-CHA.[8,14,15] In the presence of NH₃, the ions become solvated and detached from the framework, forming $Cu^{2+}(OH)^-(NH_3)_x$ mobile complexes.[8] Recently, we proposed the dry CO oxidation protocol as a viable technique to explore the formation of dinuclear Cu^{2+} structures, originating from $ZCu^{2+}(OH)^-$, under conditions representative of the low-T RHC regime over Cu-CHA. As the oxidation requires a two-electron exchange, whereas the reduction of each isolated Cu^{2+} involves one-electron transfer, CO_2 formation was suggested to signal the active participation of Cu^{2+} dimers in Cu-zeolite catalysts.[16–18] Furthermore, NH₃ adsorption prior to the CO feed greatly enhanced the CO oxidation activity.[16] This positive effect was attributed to the solvated ions' mobility, as the ions were proposed to diffuse inter the cages, forming binuclear

[a] U. Iacobone, Prof. Dr. I. Nova, Prof. Dr. E. Tronconi
     Laboratory of Catalysis and Catalytic Processes (LCCP)
     Dipartimento di Energia
     Politecnico di Milano
     Via Giuseppe La Masa 34, 20156 Milan (Italy)
     E-mail: enrico.tronconi@polimi.it
[b] Dr. R. Villamaina, Dr. M. P. Ruggeri, Dr. J. Collier, Dr. D. Thompsett
     Emission Control Department
     Johnson Matthey Technology Centre
     Blounts Court Road, Sonning Common, Reading RG4 9NH (UK)

     Supporting information for this article is available on the WWW under
     https://doi.org/10.1002/open.202200186

ChemistryOpen

Research Article
doi.org/10.1002/open.202200186

**Chemistry
Europe**
European Chemical
Societies Publishing

species capable to catalyze the CO oxidation. The dual site nature of the Cu^{2+} reduction process results are coherent with the recent RHC transient kinetic analysis over several of Cu-CHA catalysts, which revealed a rate quadratic dependency of Cu reduction on the oxidized Cu^{2+} fraction once NH_3 was pre-loaded.[19] Conversely, these findings do not reconcile with the widely proposed single-site-RHC mechanisms, suggesting the need for proposing novel, alternative pathways.[9,14,20]

Herein, we have further inspected the role of NH_3 in the formation of multinuclear Cu^{2+} species by adopting a combination of transient response methods. Dedicated tests with modulated NH_3 coverage enabled loading the different catalyst adsorption sites to varying degrees. Subsequent dry CO oxidation tests clearly titrated the active dimer-like Cu^{2+} species onset only in the presence of NH_3-ligated Cu^{2+}, whereas NH_3 adsorbed onto Brønsted sites did not significantly affect the CO oxidation process. The adopted protocols also provide information on the relative rates of NH_3 adsorption, Cu-dimer formation, and CO oxidation.
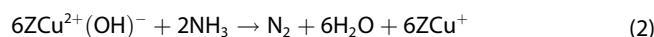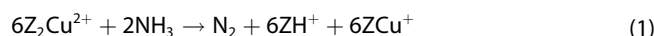
Results and Discussion

The goal of this research activity is to assess how the formation of multinuclear Cu^{2+} species is affected by the presence of NH_3 coordinated to different acidic catalytic sites of Cu-CHA, under conditions representative of low-T SCR-RHC. A deeper understanding of the NH_3 adsorption mechanism on the Cu-CHA sites is thus require, hence a series of dedicated tests have been carried out first. The details of these have been reported in the Experimental Section of this paper.
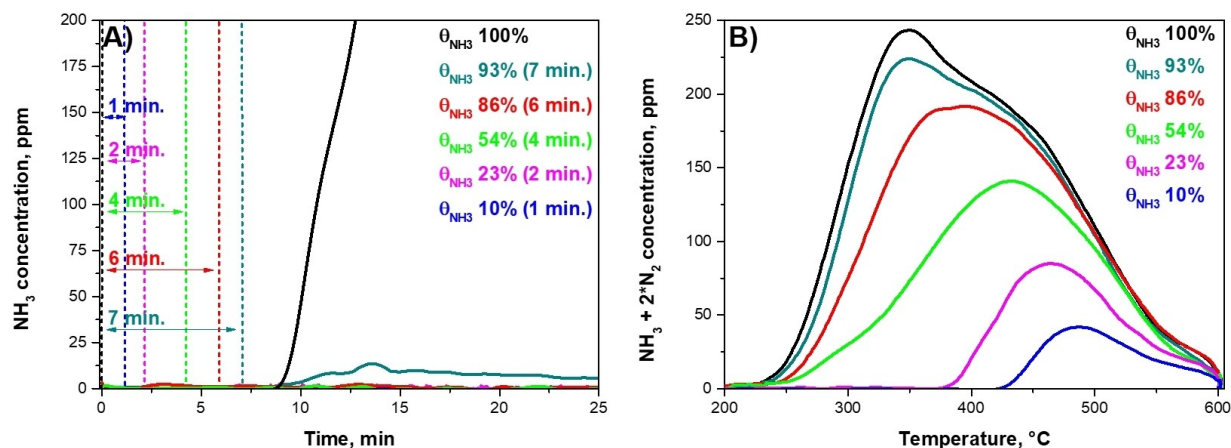
NH_3 adsorption – Variable adsorption time effect

NH_3, the primary reducing agent for NO_x in NH_3-SCR, is also extensively used in literature to titrate the acid sites of the Cu-CHA catalyst, exploiting its capacity to form chemical bonds with different strengths.[14,15] Thus, isothermal NH_3 adsorption + TPD (temperature-programmed desorption) tests allow to estimate both the total NH_3 storage and the catalyst sites involved in the adsorption process. All the tests have been herein realized under dry conditions to avoid competition of H_2O and NH_3 for adsorption on the catalyst sites, Cu^{2+} hydrolysis phenomena and other complexities.[18,21] The isothermal adsorption and desorption phases were realized in the presence of O_2 to avoid any Cu^{2+} reduction by NH_3. Since the reference CO oxidation test is performed at isothermal conditions (200°C), the same temperature has been adopted in these NH_3 adsorption tests for consistency. An initial test has been realized with full catalyst saturation: the temporal evolution of the temperature and the involved species is shown in Figure S2 (Supporting Information), while Table S1 reports the quantitative analysis generated by NH_3 and N_2 profiles integration. During the initial NH_3 feed, a dead time was observed (≈ 9 min), where all the reactant fed to the catalyst is adsorbed and no release is detected by the instruments. After

this initial phase, the NH_3 outlet concentration rapidly increased, reaching the feed concentration level at complete catalyst saturation. The cardinal phase for this work is the TPD step, which allows to evaluate the features of chemically adsorbed NH_3. It is thus realized after an isothermal desorption phase to remove the contribution of weakly adsorbed species. To avoid ammonia oxidation during the temperature ramp, the O_2 feed is cut off prior to the catalyst heating. A dual-site desorption trend is identified during the TPD, a known trait for this materials already observed in previous experimental campaigns on a variety of Cu-CHA samples with different SAR and Cu loadings.[15,21] The high-temperature peak (centred at ≈ 450°C) is associated with the NH_3 desorption from Brønsted acid sites (ZH^+), characterizing the unexchanged CHA framework, while the low-temperature feature (≈ 350°C) is ascribed to the Cu^{2+} ions' Lewis acidity (with a possible minor contribution of extra-framework Al). Concurrently with the NH_3 chemical desorption, a N_2 release is observed in the Lewis peak region. The integral nitrogen production is the result of full Cu^{2+} reduction by NH_3, according to $Cu^{2+}:N_2 = 1:6$ stoichiometries for both ions as reported in the following (Equations (1) and (2)) ($Cu^{2+}/N_2 = 4.4$ μmol/0.67 μmol = 6.6):[22,23]

$$6Z_2Cu^{2+} + 2NH_3 \rightarrow N_2 + 6ZH^+ + 6ZCu^+ \tag{1}$$

$$6ZCu^{2+}(OH)^- + 2NH_3 \rightarrow N_2 + 6H_2O + 6ZCu^+ \tag{2}$$

Accounting for this reduction process contribution, the overall integral NH_3 TPD is evaluated as the sum of the NH_3 release with twice the N_2 production (10.4 μmol). As expected, this value is lower (-36%) than the same assessed in a previous investigation where the adsorption was effected at 150°C.[15,21] In an earlier work, we have emphasized the correlation between the Lewis desorption feature and the ammonia coordination of the copper ions, performing an analysis of the NH_3/Cu ratio.[21] This is typically used as a Cu^{2+} speciation index for Cu-CHA catalysts; however, depending on the gas phase conditions, different numbers of NH_3 ligands can be present on the Cu^{2+} ions. Lewis-NH_3/Cu shows a range between 3–4 when NH_3 is present in the gas phase (forming $Cu^{2+}(OH)^-(NH_3)_3$ and $Cu^{2+}(NH_3)_4$), while it decreases to 1–2 when gaseous ammonia is removed ($Cu^{2+}(OH)^-(NH_3)$, $Cu^{2+}(NH_3)_2$).[8,21] Recently, we showed that the Lewis-NH_3/Cu ratio of different Cu-CHA catalysts, assessed by deconvolution of the TPD curves, was in agreement with the expected number of ligands on $ZCu^{2+}(OH)^-$ and Z_2Cu^{2+}.[21] With this knowledge, we replicated the NH_3 adsorption tests, changing the NH_3 injection phase duration to evaluate the impact of the adsorption sites fractional coverage on the TPD phase. In the previous test with complete catalyst saturation, NH_3 breakthrough occurred after an initial 9 min dead time. Thus, we chose reduced duration feed times of 1, 2, 4, 6 and 7 min. The respective isothermal NH_3 adsorption and desorption phases are depicted in Figure 1A. Up to 6 min, no desorption was detected, with a minor release occurring at 7 min. Consequently, all the NH_3 fed is directly stored on the catalyst. The corresponding TPD traces are plotted in Figure 1B as $NH_3 + 2*N_2$, alongside the TPD trace collected after full

ChemistryOpen

Research Article
doi.org/10.1002/open.202200186

Chemistry Europe
European Chemical
Societies Publishing

Figure 1. Comparison of NH_3 adsorption/desorption phases with variable adsorption time (A), and the relative $NH_3 + 2*N_2$ TPD (B). $NH_3 = 500-0$ ppm, $O_2 = 8-0\%$ v/v, $H_2O = 0\%$ v/v, balanced in He. GHSV = 266250 $cm^3/h/g_{cat}$ (STP) ($W_{cat} = 16$ mg). $T = 190-600\,^{\circ}C$, heating rate = $15\,^{\circ}/min$. Pre-oxidized catalyst.

Table 1. Quantitative analysis of the TPD phase, with the evaluation of NH_3 coverage (θ_{NH3}) for each adsorption time.

| Variable NH_3 ads. time [min]	TPD: $NH_3 + 2*N_2$ [μmol]	θ_{NH3} [%]
Saturation	10.4	100
7	9.7	93
6	9.0	86
4	5.6	54
2	2.4	23
1	1.0	10

saturation. A single high-temperature peak is detected considering 1 and 2 min of adsorption time, while only at 4 min the Lewis NH_3 feature starts to appear. The Brønsted acid sites reach nearly complete saturation at 6 min, while the low-temperature acidity proceeds to continuously increase. Accounting for the global NH_3 adsorption mechanism on Cu-CHA materials, this data set clearly points out how the Brønsted acid sites are saturated first, while NH_3 coordinates to the Lewis sites only later on, as the weak adsorption sites are expected to be saturated last. Table 1 reports the quantitative analysis of the TPD traces for different adsorption times. Considering the trace after full NH_3 saturation as reference, the NH_3 loading (θ_{NH3}) is defined as the ratio between the TPD at a specific adsorption time with respect to full saturation conditions. On comparing Table 1 with Figure 1, it is possible to conclude that the solvation of the Cu^{2+} sites only initiates at NH_3 loadings higher than 50%, while, at lower θ_{NH3} values, their contribution to the NH_3 storage can be considered as negligible.

CO oxidation – Variable NH_3 loading effect

The dry CO oxidation protocol has been already applied to the sample herein employed, and the temporal evolution of the global species has been reported elsewhere. [17] A net positive effect on CO_2 formation was observed when the catalyst was fully saturated with NH_3 prior to the CO feed.[17] The same tests, with and without NH_3, have been replicated: when CO reaches the catalyst, a transient CO_2 production is detected (shown in
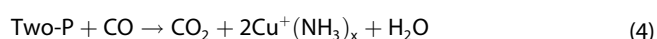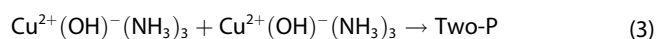
Figure 2) with a characteristic initial peak and a slow decreasing trend. The presence of NH_3 ($\theta_{NH3} = 100\%$) clearly enhances the process with respect to its absence ($\theta_{NH3} = 0\%$), in agreement with previous findings.

As anticipated in the Introduction section, the NH_3-assisted CO-to-CO_2 dry oxidation protocol has been recently proposed as a clean and effective probe reaction for multinuclear Cu^{2+} species in Cu-CHA catalysts.[16–18] This reaction involves a two-electron transfer process with an oxygen-donor species, while
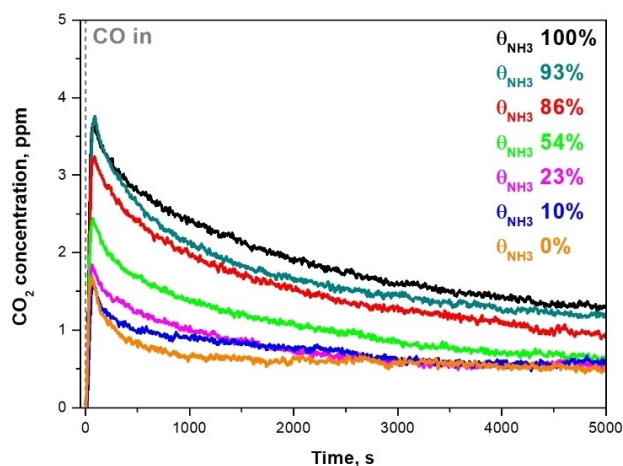
Figure 2. CO_2 released during the CO oxidation phase with different NH_3 loadings. Feed: CO = 1000 ppm, $O_2 = 0\%$ v/v, $H_2O = 0\%$ v/v, balanced in He. GHSV = 266250 $cm^3/h/g_{cat}$ (STP) ($W_{cat} = 16$ mg). $T = 200\,^{\circ}C$. Pre-oxidized catalyst.

ChemistryOpen

Research Article
doi.org/10.1002/open.202200186

**Chemistry
Europe**
European Chemical
Societies Publishing

the Cu^{2+}-to-Cu^+ reduction requires exchange of a single electron. Thus, dinuclear Cu^{2+} complexes necessarily result to catalyze CO oxidation; furthermore, $ZCu^{2+}(OH)^-$ is the only Cu cation with a removable oxygen, suggesting it as the sole precursor of catalytic centers for CO oxidation. Dynamic simulations indicate the formation of such structures to occur during the NH_3 adsorption phase: as mentioned earlier, the presence of NH_3 ligands provides the $Cu^{2+}(OH)^-(NH_3)_3$ complex with the ability to inter-cage diffuse.[8] DFT has shown that, under these conditions, an exergonic pairing process is favored: two $Cu^{2+}(OH)^-(NH_3)_3$ can cohabit the same CHA cage in a two-proximate configuration (Two-P).[24] The two main process steps can be summarized according to the following Equations (3) and (4):
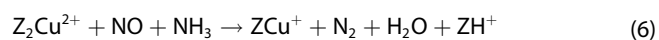
$$Cu^{2+}(OH)^-(NH_3)_3 + Cu^{2+}(OH)^-(NH_3)_3 \rightarrow \text{Two-P} \qquad (3)$$

$$\text{Two-P} + CO \rightarrow CO_2 + 2Cu^+(NH_3)_x + H_2O \qquad (4)$$

The involvement of $ZCu^{2+}(OH)^-$ ions has been verified by a second order kinetic analysis of CO oxidation on Cu-CHA catalysts with variable SAR and Cu loading.[17] Besides, the integral CO_2 production analysis points to an expected asymptotic value which is in close agreement with the $ZCu^{2+}(OH)^-$ population half.[18] An independent UV-Vis analysis verified how exposure of $ZCu^{2+}(OH)^-$-rich catalysts to CO resulted in a significant reduction of the associated UV bands, while negligible changes were observed on a sample with a predominant population of Z_2Cu^{2+}. In fact, molecular dynamic simulations show that the Z_2Cu^{2+} intra-cage mobility is limited even in the presence of NH_3; their reactivity has been observed only as a result of hydrolysis phenomena, not active here.[8,9,18] The dry CO oxidation proceeds, therefore, according to a dual-site mechanism involving isolated $ZCu^{2+}(OH)^-$ species, precursors of the Two-P complex, whose dynamic formation by NH_3 solvation plays a critical role in the process.

The integral CO_2 production is reported in Table 2. Using the values reported therein, it is possible to estimate the $ZCu^{2+}(OH)^-$ reduction extent, ($ZCu^{2+}(OH)^-$ red.) defined as twice the CO_2 release with respect to the total ion population. Clearly, the presence of NH_3 pre-adsorbed on the catalyst enhances the reduction up to 3 times with respect to its absence (47.3% vs. 16.4%), due to the NH_3 mobilizing effect. Noteworthily, even under fully NH_3 saturated conditions, we never reached the complete site reduction within the 90 min duration of the phase. Indeed, the CO oxidation is a slow process, and the CO_2

signal never approached the zero level under any of the considered conditions.

The dry CO oxidation protocol has been further replicated varying the NH_3 adsorption time, as described in the Experimental Section. This procedure allows to assess the effect of different initial NH_3 coverages on the CO oxidation activity, as well as the role of different adsorption sites. The new CO_2 evolution data set is plotted in Figure 2. Limited NH_3 loadings ($\theta_{NH3} = 10\%$ and 23%) result in CO_2 profiles almost overlapping with the zero-loading test. This is coherent with the corresponding NH_3-TPD curves, since at such low coverages, NH_3 is expected to primarily bind to Brønsted acid sites, therefore being unable to mobilize the Cu^{2+} ions and to thus promote the CO-to-CO_2 oxidation. A remarkable CO_2 release increment is appreciated in correspondence to the Lewis feature onset at $\theta_{NH3} = 54\%$, ascribed to the progressive $ZCu^{2+}(OH)^-$ solvation. At $\theta_{NH3} = 93\%$, we reach a profile close to the full saturation condition ($\theta_{NH3} = 100\%$), corresponding to a nearly entire mobilization of the cation population. The analysis of the $ZCu^{2+}(OH)^-$ reduction extent leads to similar conclusions: from zero to low NH_3 loadings, the estimated fraction is scarcely affected by the reactant presence (16.4–20.0%), while a significant extent can be appreciated (26.4–47.3%) concurrently to the coordination of the Cu^{2+} ions by NH_3. These findings are consistent with the proposed dry CO oxidation protocol interpretation, and further validate the central role of NH_3 in the formation of Cu^{2+} pairs (Two-P) originating from $ZCu^{2+}(OH)^-$. Following the CO oxidation phase, a final $NO + NH_3$ titration is performed to close the Cu^{2+} balance. The well-established Cu^{2+} reduction chemistry over Cu-CHA is represented by the reported reactions (Equations (5) and (6)):[9,15,19,25]
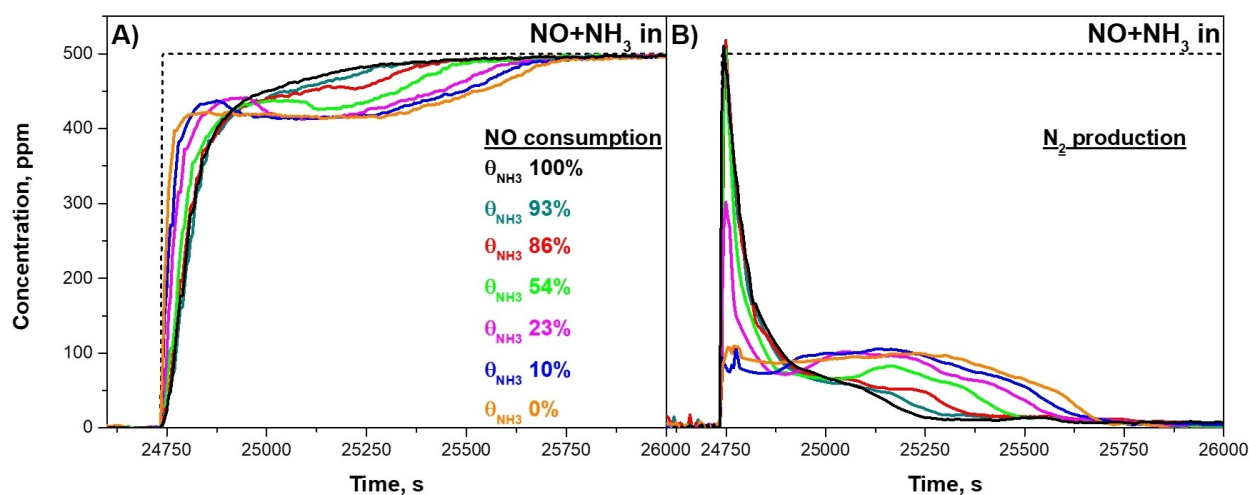
$$ZCu^{2+}(OH)^- + NO + NH_3 \rightarrow ZCu^+ + N_2 + 2H_2O \qquad (5)$$

$$Z_2Cu^{2+} + NO + NH_3 \rightarrow ZCu^+ + N_2 + H_2O + ZH^+ \qquad (6)$$

The equimolar stoichiometries ($Cu^{2+}:NO:N_2 = 1:1:1$) permit the direct quantification of the reduced Cu^{2+} by integrating the temporal NO consumption and N_2 production traces. Table S2 reports these values, and a good match between the two integrals is always verified ($NO/N_2 \approx 1$). Remarkably, the reduction dynamics are clearly affected by the variable θ_{NH3}, as apparent in Figure 3. Recently, a RHC transients kinetic study on Cu-CHA catalysts with pre-adsorbed NH_3 pointed out a second order reduction rate in the oxidized Cu^{2+} fraction.[19] Comparable transients are observed here considering $\theta_{NH3} = 100\%$, where 500 ppm of N_2 are detected upon co-feeding NO and

Table 2. Integral CO_2 production and $ZCu^{2+}(OH)^-$ fraction reduced by CO for different initial NH_3 coverages (θ_{NH3}).

| CO oxidation tests – variable θ_{NH3} [%]	CO_2 release [µmol]	$ZCu^{2+}(OH)^-$ red. [%]
100	0.52	47.3
93	0.49	44.5
86	0.43	39.1
54	0.29	26.4
23	0.22	20.0
10	0.21	19.1
0	0.18	16.4

ChemistryOpen

Research Article
doi.org/10.1002/open.202200186

Chemistry Europe
European Chemical
Societies Publishing

Figure 3. NO (A) and N_2 (B) evolution during the $NO + NH_3$ feed, with different NH_3 loadings. $NO + NH_3$ feed: $NH_3 = NO = 500$ ppm, $CO = 0$ ppm, $O_2 = 0\%$ v/v, $H_2O = 0\%$ v/v, balanced in He. GHSV $= 266250$ cm^3/h/g$_{cat}$ (STP) (W$_{cat} = 16$ mg). $T = 200\,°C$. Pre-oxidized catalyst.

NH_3, followed by a rapid decrease (Figure 3B); the NO consumption shows a mirror-like trend (Figure 3A). Different initial NH_3 loadings, however, determine a net profile alteration. Absent or scarce NH_3 ($\theta_{NH3} = 0$–23%) inhibits the reduction process, with a plateau feature corresponding to an approximately constant production of 100 ppm of N_2. NO readily reacts with Cu^{2+}-NH_3, as shown by both an independent spectroscopic study and our previous work on NH_3 reactivity on Cu-CHA; hence, the slow reduction observed here could be ascribed to the NH_3 adsorption time required on the Cu^{2+} sites.[25,26] As the loading increases ($\theta_{NH3} = 54$–93%), the reduction process results improved with a clear net N_2 production peak, coherently with the wider fraction of solvated Cu^{2+} ions. Therefore, these trends show strong similarities with the CO_2 evolution previously observed. The CO_2 trace integrals (counted twice) and the averaged NO consumption/N_2 production traces can be used to assess the extents of the two Cu^{2+} reduction processes, that is, by CO and by $NO + NH_3$, combined with the knowledge of the sample total Cu^{2+} content. The estimated reduced Cu^{2+} fractions are reported in Table S2 and plotted against θ_{NH3} in Figure 4 (Cu^{2+} red. by CO or by $NO + NH_3$) alongside the overall Cu^{2+} balance, computed as their sum, which is closed with a maximum error of 2%. The limited reduction extent by CO (8.2– 10.0%) al low NH_3 coverages ($\theta_{NH3} = 0$–23%) is verified by the $NO + NH_3$ titration, which assesses a Cu^{2+} high oxidation state (89.3–92.0%). In agreement with the previous considerations, the NH_3 coordination on Cu^{2+} is crucial for the Cu-CHA reduction processes; consequently, we observe relevant changes starting from a half coverage condition ($\theta_{NH3} = 54\%$), when Lewis sites begin to be active in the ammonia adsorption. Between $\theta_{NH3} = 54$ and 93%, the Cu^{2+} fraction reduced by CO grows from 13.2 to 23.6%, close to the full saturation conditions; correspondingly, the final $NO + NH_3$ reduction titrates a constantly decreasing fraction of oxidized copper, nicely closing the Cu^{2+} balance.
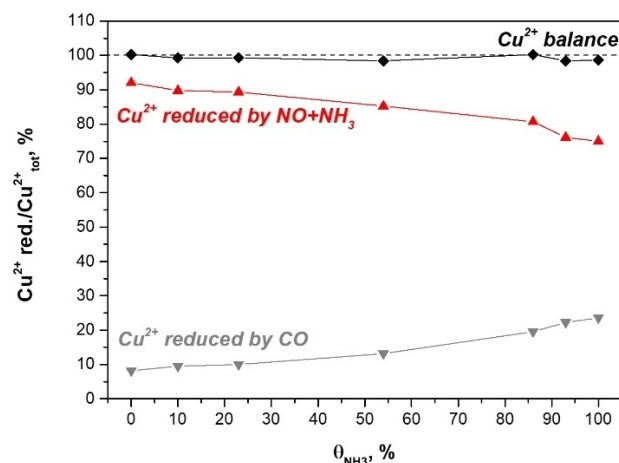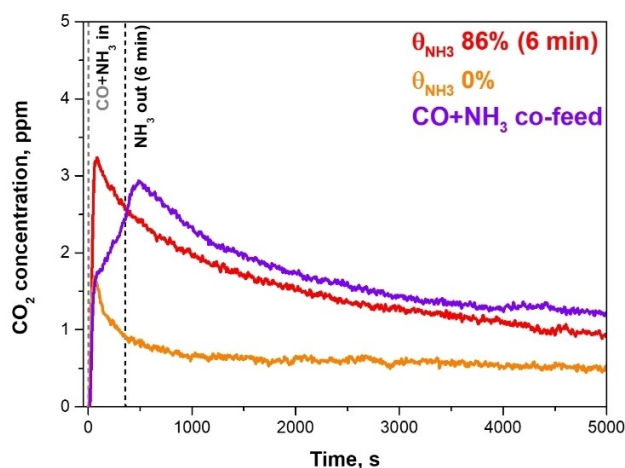

Figure 4. Fraction of Cu^{2+} reduced by CO (gray) and by $NO + NH_3$ (red) during CO oxidation tests with different NH_3 loadings. The overall Cu^{2+} balance (black) is also shown.

CO oxidation – CO and NH_3 co-feed

As discussed, two phenomena concur during the NH_3 adsorption phase, namely the saturation of the catalyst sites by NH_3 and the formation of the Two-P structure, that is, the active Cu^{2+} structure in the CO-to-CO_2 oxidation. When co-feeding NH_3 and CO on a clean catalyst, the two processes proceed concurrently with the Two-P reduction by CO, thus enabling a preliminary assessment of the relative rates of the reaction cascade. To prevent any Cu^{2+} reduction by gas phase NH_3 and to obtain data directly comparable to the previous analysis, this test has been run applying a limited NH_3 saturation time. Figure 5 depicts the CO_2 evolution from the co-feed experiment with 6 min of NH_3 adsorption, compared to the reference test.

Once CO and NH_3 reach the catalyst, the co-feed experiment trace shows an overlapping trend with the zero-loading test ($\theta_{NH3} = 0\%$) during the very first minutes. Without ammonia, the mobility of $ZCu^{2+}(OH)^-$ is limited and a negligible dimer

ChemistryOpen

Research Article
doi.org/10.1002/open.202200186

Chemistry Europe
European Chemical
Societies Publishing

Figure 5. CO_2 evolution during the $CO+NH_3$ co-feed test, where NH_3 is removed after 6 min. $CO+NH_3$ co-feed: $NH_3 = 500$ ppm (6 min), $NO = 0$ ppm, $CO = 1000$ ppm, $O_2 = 0\%$ v/v, $H_2O = 0\%$ v/v, balanced in He. GHSV = 266250 cm³/h/g_cat (STP) ($W_{cat} = 16$ mg). $T = 200\,°C$. Pre-oxidized catalyst.

formation, with a correspondingly slight CO oxidation activity, is expected. However, as the co-feed test proceeds, the CO_2 signal grows; indeed, during this phase, the Two-P formation is favored due to the ammonia solvation effect and it becomes faster than the competing reduction by CO. A maximum is reached after 6 min of NH_3-feed (≈ 8 min), suggesting that the coupling of the Cu^{2+} ions is slower than the actual NH_3 adsorption. Beyond this point, no more Two-P formation is expected, the CO_2 evolution results akin to the previous analyzed profiles and parallel to the trend collected with a 6 min NH_3 pre-adsorption phase, with comparable integral values (0.48 μmol). Similar findings have been observed when replicating the protocol with a 7 min feed of NH_3 as shown in Figure S3. From this data set we propose the ammonia adsorption to be faster than the Two-P formation process, while the CO oxidation turns out to be the slowest of the involved phenomena.

Conclusions

We have addressed the role of NH_3 during the low-T RHC-SCR on a Cu-CHA catalyst using transient response methods. A dedicated methodology has clearly shown that NH_3 is adsorbed onto the Brønsted zeolite sites in the initial phase of the adsorption process, while the Lewis sites, extensively proved to be associated with the Cu^{2+} ions, become solvated at higher degrees of loading. Once coordinated with NH_3 ligands, ZCu^{2+} $(OH)^-$ becomes inter-cage mobile and a thermodynamic driving force exists to enable its coupling with an adjacent complex in the same zeolite cage, forming a two-proximate structure (Two-P). This is regarded as the catalytic active site for the CO-to-CO_2 oxidation, a clean probe reaction for the detection of dinuclear Cu^{2+} complexes. In this work, we have run dry CO oxidation tests preceded by a modulated NH_3 adsorption, to replicate the loading and solvation conditions assessed in a previous NH_3

adsorption study. Remarkably, significant CO_2 production has been detected only when the Cu^{2+} sites were partially solvated (Lewis-NH_3), coherently with the formation of Two-P complexes. The Brønsted-NH_3 instead was unable to catalyze the CO oxidation process. Similar features were observed during the following and final $NO+NH_3$ titration phase: the presence of NH_3-Cu^{2+} is crucial to enable the reduction dynamics with the characteristic second order dependence on oxidized Cu^{2+} assessed in a dedicated transient kinetic study. Finally, based on $CO+NH_3$ co-feed experiments, we preliminarily propose that the NH_3 adsorption process proceeds more rapidly than the Two-P formation, both processes being faster than CO oxidation.

The present work further emphasizes the central role of NH_3-Cu^{2+} complexes in the low-T SCR mechanism over Cu-CHA and validates the use of dry CO oxidation as an effective transient method to titrate the formation of dinuclear Cu^{2+} complexes (Two-P) during RHC conditions. The dual-site nature of the Cu^{2+} reduction process corroborates the previously established mechanistic understanding for these systems.

Experimental Section

Catalyst characterization

The experimental campaign for this study was carried out on one research catalyst sample, a Cu-exchanged chabazite (Cu-CHA) in the form of powder, supplied by Johnson Matthey. The catalyst has been characterized in previous work by transient response methods and quantitative analyses.[15] $NO+NH_3$-TPR, H_2-TPR and ICP-MS analysis assigned a Cu loading of 1.7% w/w (0.2750 mmol g$^{-1}_{cat}$), confirming the equivalence between the amount of reducible Cu and the total Cu loading in the zeolite. The absence of CuO_x species or unexchanged Cu was confirmed by UV-Vis spectra. The SiO_2/Al_2O_3 (SAR) and the Cu/Al ratios resulted respectively equal to 10 and 0.12. NO_2 adsorption, followed by temperature programmed desorption, was used to evaluate a $ZCu^{2+}(OH)^-$ fraction of 50% (0.1375 mmol g$^{-1}_{cat}$), further confirmed by deconvolution of the H_2-TPR profile.[15]

Experimental set-up

A quartz microflow reactor (internal diameter ≈ 6 mm) was loaded with 16 mg of Cu-CHA catalyst, diluted with cordierite up to 130 mg, with 90 microns as average particle size for both. The catalyst bed was suspended by means of quartz wool, preceded, and followed by quartz grains to enhance gas phase mixing. A K-type thermocouple, directly in contact with the catalyst bed, was used to monitor the temperature evolution. The reactor was placed in a vertical electric oven, set in an experimental rig where Helium was used as balance gas. Mass flow controllers (Brooks Instruments) were used to dose the reactant gas species. Argon acted as tracer gas, and two fast 6-way valves guaranteed step changes of NO, NH_3, CO feed concentration, while the oxygen flow was regulated acting on the related mass flow controller. A saturator was used to feed water vapor and its concentration was adjusted by controlling the saturator temperature according to Antoine's Law. The temporal evolution of the gas species from the reactor outlet was followed by a UV+IR analyzer (ABB: LIMAS11 HW+URAS26) and a mass spectrometer (QGA Hiden Analytical), set in a parallel configuration, enabling the simultaneous measurement of all the

ChemistryOpen

Research Article
doi.org/10.1002/open.202200186

**Chemistry
Europe**

European Chemical
Societies Publishing

species involved: CO, CO_2, NH_3, NO, NO_2, N_2, N_2O, O_2, H_2O and Ar. The catalyst was initially hydrothermally preconditioned at 600 °C in the presence of 10% v/v of O_2 and H_2O for 5 h to ensure catalyst cleaning. Prior to each test, the sample was treated at 550 °C with 8% v/v of O_2 for 1 h: this phase was used to remove previously adsorbed species and ensure complete catalyst oxidation. A cool-down step, in the same gas feed, was realized to reach the operative temperature of the test. Three different experimental protocols were adopted for this study as illustrated in Figure S1, with a space velocity of 266250 $cm^3/h/g_{cat}$ (STP).

Isothermal NH_3 adsorption+TPD tests

Isothermal NH_3 adsorption tests, with variable duration of the adsorption phase, followed by temperature programmed desorption (TPD), were used to study the interaction between NH_3 molecules and the catalyst adsorption sites; the experimental protocol is depicted in Figure S1A. Ammonia adsorption was realized by feeding 500 ppm of NH_3 in the presence of 8% v/v of O_2 at 200 °C, considering different injection time intervals: 1, 2, 4, 6, 7 min and up to complete catalyst saturation (1 h). The catalyst was then purged in O_2 till NH_3 concentration was below 5 ppm, to ensure the desorption of weakly bonded ammonia. A purge in He of 10 min only, with a cooling phase down to 190 °C, was used to guarantee complete O_2 removal. During the following TPD part, the temperature was linearly increased in time up to 600 °C with a heating rate of 15°/min to release the strongly adsorbed NH_3 molecules. An additional N_2 release was observed associated with the Cu reduction by NH_3.

Isothermal CO oxidation tests

The effect of variable NH_3 loading on the formation of multinuclear Cu species was studied by isothermal CO oxidation tests with different adsorption times (Figure S1B). An initial step of isothermal NH_3 injection, with 500 ppm of NH_3 with 8% v/v of O_2, followed by an isothermal desorption, was realized. The same conditions were employed and adapted for the NH_3 adsorption/desorption tests. Note that, when considering zero NH_3 loading, this whole phase was neglected. A 15 minute He-only purge was realized prior to the CO oxidation phase, where 1000 ppm of CO were fed for 90 min. Here, a transient CO_2 release was recorded, associated with the multinuclear Cu^{2+} species reduction. Following a 30 minute purge, $NO+NH_3$ titration was used to evaluate the residual Cu^{2+} fraction, co-feeding 500 ppm of NO and NH_3 for 1 h. During this phase, the N_2 formation is observed, as the product of the Cu^{2+} reduction process. No production of further N-species (N_2O, NO_2) was observed, as shown in a previous work.[19] All the protocol steps were realized at 200 °C. Isothermal CO and NH_3 co-feed tests (Figure S1C) were realized to evaluate the competition between the multinuclear Cu^{2+} species formation and their reduction. After a 15-minute purge in He, the reactor was co-fed with 1000 ppm of CO, for 90 min, and 500 ppm of NH_3, removed after 6 or 7 min. After a 30 minute purge in He, a final $NO+NH_3$ titration was carried out co-feeding 500 ppm of NO and NH_3 for 1 h.

Supporting Information Summary

Detailed steps of the experimental protocol, material balances and the 7 minute NH_3 feed Protocol C replica.

[1] A. M. Beale, F. Gao, I. Lezcano-Gonzalez, C. H. F. Peden, J. Szanyi, *Chem. Soc. Rev.* **2015**, *44*, 7371–7405.
[2] E. Borfecchia, P. Beato, S. Svelle, U. Olsbye, C. Lamberti, S. Bordiga, *Chem. Soc. Rev.* **2018**, *47*, 8097–8133.
[3] M. P. Ruggeri, I. Nova, E. Tronconi, J. E. Collier, A. P. E. York, *Top. Catal.* **2016**, *59*, 875–881.
[4] F. Gao, N. M. Washton, Y. Wang, M. Kollár, J. Szanyi, C. H. F. Peden, *J. Catal.* **2015**, *331*, 25–38.
[5] K. Leistner, O. Mihai, K. Wijayanti, A. Kumar, K. Kamasamudram, N. W. Currier, A. Yezerets, L. Olsson, *Catal. Today* **2015**, *258*, 49–55.
[6] T. V. W. Janssens, H. Falsig, L. F. Lundegaard, P. N. R. Vennestrøm, S. B. Rasmussen, P. G. Moses, F. Giordanino, E. Borfecchia, K. A. Lomachenko, C. Lamberti, S. Bordiga, A. Godiksen, S. Mossin, P. Beato, *ACS Catal.* **2015**, *5*, 2832–2845.
[7] F. Gao, E. D. Walter, M. Kollar, Y. Wang, J. Szanyi, C. H. F. Peden, *J. Catal.* **2014**, *319*, 1–14.
[8] C. Paolucci, A. A. Parekh, I. Khurana, J. R. Di Iorio, H. Li, J. D. Albarracin Caballero, A. J. Shih, T. Anggara, W. N. Delgass, J. T. Miller, F. H. Ribeiro, R. Gounder, W. F. Schneider, *J. Am. Chem. Soc.* **2016**, *138*, 6028–6048.
[9] C. Paolucci, I. Khurana, A. A. Parekh, S. Li, A. J. Shih, H. Li, J. R. Di Iorio, J. D. Albarracin-Caballero, A. Yezerets, J. T. Miller, W. N. Delgass, F. H. Ribeiro, W. F. Schneider, R. Gounder, *Science* **2017**, *357*, 898–903.
[10] A. Marberger, A. W. Petrov, P. Steiger, M. Elsener, O. Kröcher, M. Nachtegaal, D. Ferri, *Nat. Catal.* **2018**, *1*, 221–227.
[11] W. P. Partridge, S. Y. Joshi, J. A. Pihl, N. W. Currier, *Appl. Catal. B* **2018**, *236*, 195–204.
[12] C. Liu, H. Kubota, T. Amada, K. Kon, T. Toyao, Z. Maeno, K. Ueda, J. Ohyama, A. Satsuma, T. Tanigawa, N. Tsunoji, T. Sano, K. ichi Shimizu, *ChemCatChem* **2020**, *12*, 3050–3059.
[13] J. H. Kwak, H. Zhu, J. H. Lee, C. H. F. Peden, J. Szanyi, *Chem. Commun.* **2012**, *48*, 4758–4760.
[14] J. Luo, F. Gao, K. Kamasamudram, N. Currier, C. H. F. Peden, A. Yezerets, *J. Catal.* **2017**, *348*, 291–299.
[15] R. Villamaina, S. Liu, I. Nova, E. Tronconi, M. P. Ruggeri, J. Collier, A. York, D. Thompsett, *ACS Catal.* **2019**, *9*, 8916–8927.
[16] P. Da Costa, B. Modén, G. D. Meitzner, D. K. Lee, E. Iglesia, *Phys. Chem. Chem. Phys.* **2002**, *4*, 4590–4601.
[17] R. Villamaina, U. Iacobone, I. Nova, M. P. Ruggeri, J. Collier, D. Thompsett, E. Tronconi, *ChemCatChem* **2020**, *12*, 3843–3848.
[18] W. Hu, U. Iacobone, F. Gramigni, Y. Zhang, X. Wang, S. Liu, C. Zheng, I. Nova, X. Gao, E. Tronconi, *ACS Catal.* **2021**, *11*, 11616–11625.
[19] F. Gramigni, N. D. Nasello, N. Usberti, U. Iacobone, T. Selleri, W. Hu, S. Liu, X. Gao, I. Nova, E. Tronconi, *ACS Catal.* **2021**, *11*, 4821–4831.
[20] F. Gao, C. H. F. Peden, *Catalysts* **2018**, *8*, 140.
[21] R. Villamaina, F. Gramigni, U. Iacobone, S. Liu, I. Nova, E. Tronconi, M. P. Ruggeri, J. Collier, A. P. E. York, D. Thompsett, *Catalysts* **2021**, *11*, 759.
[22] E. Borfecchia, C. Negri, K. A. Lomachenko, C. Lamberti, T. V. W. Janssens, G. Berlier, *React. Chem. Eng.* **2019**, *4*, 1067–1080.

[23] F. Giordanino, E. Borfecchia, K. A. Lomachenko, A. Lazzarini, G. Agostini, E. Gallo, A. V. Soldatov, P. Beato, S. Bordiga, C. Lamberti, *J. Phys. Chem. Lett.* **2014**, *5*, 1552–1559.

[24] W. Hu, T. Selleri, F. Gramigni, E. Fenes, K. R. Rout, S. Liu, I. Nova, D. Chen, X. Gao, E. Tronconi, *Angew. Chem. Int. Ed.* **2021**, *13*, 7197–7204.

[25] N. Usberti, F. Gramigni, N. D. Nasello, U. Iacobone, T. Selleri, W. Hu, S. Liu, X. Gao, I. Nova, E. Tronconi, *Appl. Catal. B* **2020**, *279*, 119397.

[26] V. Rizzotto, D. Chen, B. M. Tabak, J. Y. Yang, D. Ye, U. Simon, P. Chen, *Chemosphere* **2020**, *250*, 126272.